



Kinetics of lipid mixing between bicelles and nanolipoprotein particles



Ginny Lai^{a,1}, Kevin Muñoz Forti^b, Robert Renthal^{a,c,*}

^a Biology Department, University of Texas at San Antonio, San Antonio, TX 78249, USA

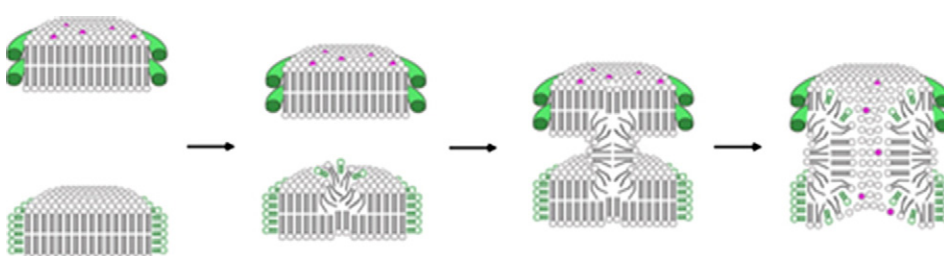
^b Biology Department, University of Puerto Rico, Ponce, PR, USA

^c Biochemistry Department, University of Texas Health Science Center, San Antonio, TX 78229, USA

HIGHLIGHTS

- Nanolipoprotein particle lipid mixing kinetics with bicelles was slow and sigmoidal.
- Short-chain lipids mixed rapidly with nanolipoprotein particles.
- Added apolipoprotein had little effect on the kinetics.
- The reaction had a high activation energy.
- Nanolipoprotein particle lipids may mix with bicelles via fusion pores.

GRAPHICAL ABSTRACT



ARTICLE INFO

Article history:

Received 28 November 2014

Received in revised form 18 January 2015

Accepted 18 January 2015

Available online 23 January 2015

Keywords:

Nanolipoprotein particle

Bicelle

Stopped flow

Fluorescence resonance energy transfer

Sigmoid kinetics

Membrane fusion

ABSTRACT

Nanolipoprotein particles (NLPs), also known as nanodiscs, are lipid bilayers bounded by apolipoprotein. Lipids and membrane proteins cannot exchange between NLPs. However, the addition of bicelles opens NLPs and transfers their contents to bicelles, which freely exchange lipids and proteins. NLP–bicelle interactions may provide a new method for studying membrane protein oligomerization. The interaction mechanism was investigated by stopped flow fluorometry. NLPs with lipids having fluorescence resonance energy transfer (FRET) donors and acceptors were mixed with a 200-fold molar excess of dihexanoyl phosphatidylcholine (DHPC)/dimyristoyl phosphatidylcholine (DMPC) bicelles, and the rate of lipid transfer was monitored by the disappearance of FRET. Near or below the DMPC phase transition temperature, the kinetics were sigmoidal. Free DHPC and apolipoprotein were ruled out as participants in autocatalytic mechanisms. The NLP–bicelle mixing rate showed a strong temperature dependence (activation energy = 28 kcal/mol). Models are proposed for the NLP–bicelle mixing, including one involving fusion pores.

© 2015 Elsevier B.V. All rights reserved.

1. Introduction

Small lipid bilayer discs are widely used to study integral membrane proteins in a membrane-like environment. Bicelles are mixtures of bilayer-forming phospholipids combined with detergents that cover the exposed lipid hydrocarbon chains of the bilayer edge. The

detergents can be either micelle-forming short-acyl-chain lipids or bile salts. Bicelles are polymorphic, but when the bilayer lipid to detergent mole ratio (q) is less than ~ 1 , bicelles consist of bilayer discs [1,2]. Nanolipoprotein particles (NLPs), also known as nanodiscs, are bilayer discs with apolipoproteins covering the hydrocarbon edges [3,4]. Membrane proteins and lipids can exchange between bicelles, but they cannot move from one NLP to another, presumably because of the apolipoprotein barrier. However, the addition of bicelles to NLPs opens them, and the NLP lipids and proteins transfer to bicelles [5]. Membrane proteins can be inserted into NLPs by cell-free protein synthesis [6]. By manipulating steric and stoichiometric factors in cell-free protein synthesis, it should be possible to prepare predominantly

* Corresponding author at: Department of Biology, University of Texas at San Antonio, 1 UTSA Circle, San Antonio, TX 78249, USA. Tel.: +1 210 458 5452.

E-mail address: robert.renthall@utsa.edu (R. Renthal).

¹ Present address: Department of Medicine, University of Florida College of Medicine, Gainesville, FL 32610, USA.

monomeric membrane proteins in NLPs. Thus, the bicelle-induced transfer process may provide a new method for studying membrane protein oligomerization [5].

The mechanism of the interaction between NLPs and bicelles is unknown. Because bicelles are in equilibrium with detergent monomers [1,7], trace amounts of mixed micelles could transport NLP lipids and proteins to bicelles. Alternatively, the NLP apolipoprotein, in a contracted conformation [8], might transfer NLP lipids and proteins to bicelles. We have now tested the effects of bicelle detergent, apolipoprotein, and temperature on lipid transfer from NLPs to bicelles, using stopped-flow kinetics.

2. Materials and methods

2.1. Materials

1,2-Dimyristoyl-*sn*-glycero-3-phosphocholine (DMPC), 1,2-dihexanoyl-*sn*-glycero-3-phosphocholine (DHPC), 1,2-dimyristoyl-*sn*-glycero-3-phosphoethanolamine-N-(7-nitro-2-1,3-benzoxadiazol-4-yl) (NBD PE), and 1,2-dimyristoyl-*sn*-glycero-3-phosphoethanolamine-N-(lissamine rhodamine B sulfonyl) (LR-PE) were obtained from Avanti Polar Lipids (Alabaster, AL). MSP1E3D1, the NLP-forming apolipoprotein, was prepared as previously described [5] or obtained from Sigma-Aldrich (St. Louis, MO).

2.2. Bicelle and NLP preparation

Bicelles and NLPs were prepared as previously described [5]. Fluorescent lipids were incorporated into NLPs at 0.02 to 0.05 mole fraction. NLPs were purified on a Superdex 200 10/30 column (GE Healthcare, Piscataway, NJ). Final concentrations were determined by measuring absorbance spectra on an Aviv/Cary 14 spectrophotometer (Aviv Biomedical, Lakewood, NJ). Extinction coefficients used were: NBD, $2.1 \times 10^4 \text{ M}^{-1} \text{ cm}^{-1}$ at 460 nm; LR, $7.5 \times 10^4 \text{ M}^{-1} \text{ cm}^{-1}$ at 566 nm [9,10]; and MSP1E3D1, $2.94 \times 10^4 \text{ M}^{-1} \text{ cm}^{-1}$ at 280 nm (<http://sligarlab.life.uiuc.edu/nanodisc/protocols.html>). In NLPs containing fluorescent lipids, the MSP1E3D1 concentration was measured after subtracting the 280 nm absorbance due to NBD and LR as follows: NBD 280 nm absorbance was 0.086 times the 460 nm absorbance [11] and LR 280 nm absorbance was 0.139 times the 566 nm absorbance (sulforhodamine B, www.fluorophores.tugraz.at/fluorescence).

2.3. Stopped flow fluorometry

NLPs containing NBD-PE and LR-PE were mixed with DMPC/DHPC bicelles ($q = 1$) in an SFM-20 stopped flow spectrometer (Bio-Logic, Knoxville, TN). The excitation light, at 440 nm with a 10 nm slit, was from a QM4 fluorometer (PTI, Edison, NJ), via a fiber optic cable. The dequenched NBD emission was detected by an R376 photomultiplier (Hamamatsu, Bridgewater, NJ), with a 520 nm interference filter, 10 nm bandwidth (Newport Corp., Irvine, CA). NLPs were loaded into a 10 mL syringe (syringe 1) at 0.6 μM or 1.2 μM in phosphate-buffered saline (PBS, 0.137 M NaCl, 2.7 mM KCl, 10 mM Na_2HPO_4 , 1.8 mM KH_2PO_4 , pH 7.4) or 4.2 μM in tris buffer (20 mM tris, 0.1 M NaCl, pH 7.4). Bicelles were loaded into a 1 mL syringe (syringe 2) at 90 mM DMPC and 90 mM DHPC in PBS or 45 mM DMPC and 45 mM DHPC in tris buffer. Each reaction was 147 μL , mixed at a 2:1 ratio of syringe 1 to syringe 2, flowing at 1 mL/s into an FC-15 (1.5 mm pathlength) cuvette. Under these conditions, the instrument dead time was 37 ms. The syringe holders, mixing head and cuvette were held at constant temperature with a Haake K10 water bath and DC10 circulator (Thermo Fisher, Waltham, MA). The difference between the bath and syringe temperature was determined by using a thermocouple. The effect of temperature on the reaction rate was measured in 4 °C increments. The stopped flow apparatus was equilibrated for 25 min at each new temperature before making measurements.

3. Results

3.1. NLP reaction with bicelles

NLPs containing fluorescence resonance energy transfer (FRET) donor–acceptor pairs of fluorescent-tagged lipids (NBD-PE and LR-PE) were mixed with a large excess of bicelles ($q = 1$). The time dependence of the increase in dequenched NBD fluorescence (Fig. 1) was assumed to measure the rate of lipid transfer from NLPs and subsequent further transfer between bicelles. The data were fit with an empirical equation:

$$y = A(1 - \exp(-kt))^n \quad (1)$$

where y is the NBD fluorescence at time t , A is the maximum dequenched NBD fluorescence signal when all the lipids are dispersed in bicelles (proportional to the total concentration of NBD-PE), k is the pseudo-first-order rate constant, and n is a fitted parameter. The rate constant was surprisingly small (0.26 s^{-1} , lower curve, Fig. 1). This can be compared with the expected pseudo-first-order rate constant for a simple NLP–bicelle collision mechanism. The measured diffusion coefficient for bicelles [12] is $4 \times 10^{-7} \text{ cm}^2/\text{s}$. Combined with the measured radii of bicelles and NLPs [5], this suggests a second-order rate constant in the range of $10^9 \text{ M}^{-1} \text{ s}^{-1}$ [13] for a reaction mechanism with the rate-limiting step for lipid transfer involving simple collisions between NLPs and bicelles. Since the bicelle concentrations ($\approx 0.2 \text{ mM}$) were in large excess over the NLP concentrations ($\approx 1 \mu\text{M}$), the expected pseudo-first-order rate constant for a collision mechanism would be in the range of $2 \times 10^5 \text{ s}^{-1}$.

The kinetic curves displayed a sigmoid shape, which Eq. (1) represents by using the exponent n ($n = 1.6$ in Fig. 1). Sigmoid reaction kinetics can indicate an autocatalytic mechanism. Eq. (1) fits the experimental data with correlation coefficients greater than 0.99. However, when very high concentrations of NLPs were used (Fig. 1, upper curve), a burst phase was observed in the first several hundred milliseconds. The magnitude of the burst phase was less than 4% of the final NBD fluorescence. Thus it could not be observed at low concentrations, where there was a lower signal-to-noise ratio. The properties of the burst phase were not pursued in the experiments reported here.

Initial rates of fluorescent lipid mixing were estimated from Fig. 1 and are given in Table 1. When the NLP concentration was doubled,

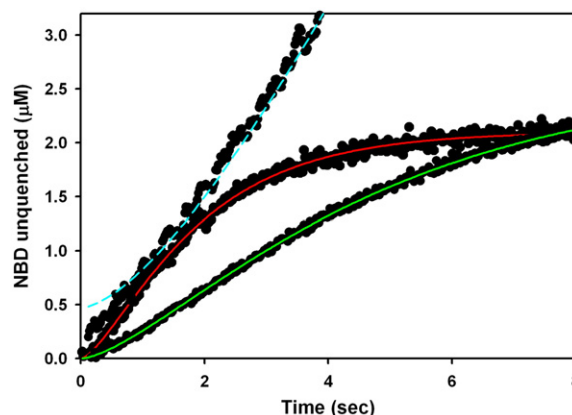


Fig. 1. Kinetics of bicelle-induced opening of nanolipoprotein particles (NLPs), measured by the disappearance of fluorescence resonance energy transfer between lipids. Conditions (final concentrations): Upper: 2.8 μM NLPs, 22.9 μM 1,2-dimyristoyl-*sn*-glycerol-3-phosphoethanolamine-N-(lissamine rhodamine B sulfonyl) (LR-PE), 29.3 μM 1,2-dimyristoyl-*sn*-glycerol-3-phosphoethanolamine-N-(7-nitro-2-1,3-benzoxadiazol-4-yl) (NBD-PE), 30 mM bicelle lipid; middle: 0.4 μM NLPs, 2.6 μM LR-PE, 2.1 μM NBD-PE, 60 mM bicelle lipid; lower: 0.8 μM NLPs, 2.5 μM LR-PE, 2.6 μM NBD-PE, 60 mM bicelle lipid. Lines (Eq. (1) parameters): red, $k = 0.66 \text{ s}^{-1}$, $n = 1.6$; green, $k = 0.26 \text{ s}^{-1}$, $n = 1.6$; blue, $k = 0.07 \text{ s}^{-1}$, $n = 1.6$. Temperature, 23.6 °C.

while holding the bicelle and total fluorescent lipid concentrations the same, the initial rate decreased by roughly a factor of two. In this experiment, the same number of fluorescent lipids was spread out over twice the concentration of NLPs. The observed slower rate indicates that the mole fraction of fluorescent lipid (i.e. NBD/NLP ratio) contributes to the rate-limiting step of the reaction mechanism. When the NBD/NLP ratio was doubled and the bicelle concentration was halved, the observed rate did not change, indicating that the bicelle concentration also contributes to the rate-limiting step. (In Table 1, the bicelle concentration is indicated by the DMPC concentration; the DHPC concentration was also halved, so q was unchanged.)

3.2. Role of bicelle detergent in the NLP–bicelle reaction

Under the conditions of the kinetic experiments in Fig. 1, about half of the added DHPC was combined with DMPC in bicelles, and about half was free DHPC monomer. It is possible that the component reacting with NLPs is DHPC monomers rather than DHPC/DMPC bicelles. In order to test this, NLPs were mixed with DHPC alone at various concentrations. Above the critical micelle concentration (cmc) of DHPC (16 mM), all the NBD-PE was dequenched (presumably transferred from NLPs to DHPC micelles) at a rate faster than the instrument dead time. Below the cmc, partial dequenching of NBD was observed. The final equilibrium levels were below the level observed for DHPC micelles (Fig. 2). These equilibrium levels formed faster than the instrument dead time and were stable for 40 s (the longest time measured). This partial reaction cannot be due to bicelle formation by DHPC combining with DMPC from the NLPs, because at the low concentration of DMPC in the NLPs (0.35 mM) and the sub-cmc DHPC concentration, bicelles are not likely to form [14]. Rather, a trace concentration of DHPC micelles probably exists below the cmc and these are sufficient to solubilize some of the NBD-PE in the NLPs. For example, when DHPC was at 8.3 mM, the fluorescence quickly equilibrated at 32% of the total NBD signal. The total NBD-PE in the reaction was 2.6 μ M. To disperse 32% of this into micelles would require at least 27 μ M micellar DHPC ($0.32 \times 2.6 \mu\text{M} \times 32$ DHPC molecules per micelle), an amount well within the available 8.3 mM concentration of total DHPC. These experiments show that the rate-limiting step of the NLP–bicelle reaction does not involve the reaction of NLPs with DHPC monomers or micelles. DHPC monomers do not appear to react with NLPs, and DHPC micelles react with NLPs far faster than the observed bicelle reaction kinetics.

3.3. Role of apolipoprotein in the NLP–bicelle reaction

The apolipoprotein used in the NLPs for these experiments, MSP1E3D1, is derived from apoA1 [3]. Exchangeable apolipoproteins such as apoA1 exist in both a water-soluble form as well as a lipid-bound form. The observation of intermediate lipid-bound forms [8] suggests that MSP1E3D1 might account for the sigmoid kinetics (Fig. 1) via the following autocatalytic scheme:



Table 1

Effects of NLP and lipid concentrations on initial rates of lipid mixing.

[NLP] (μM)	Bicelle [DMPC] mM	NLP [NBD] μM	NBD/NLP	Initial rate (μM NBD/s)	Rate ratio	Bicelle [DMPC] \times [NBD]/NLP	Ratio
0.4	30	2.1	5.25	0.75	1.00	158	1.00
0.8	30	2.6	3.25	0.37	0.49	97.5	0.62
2.8	15	29.3	10.5	0.9	1.20	157	0.99

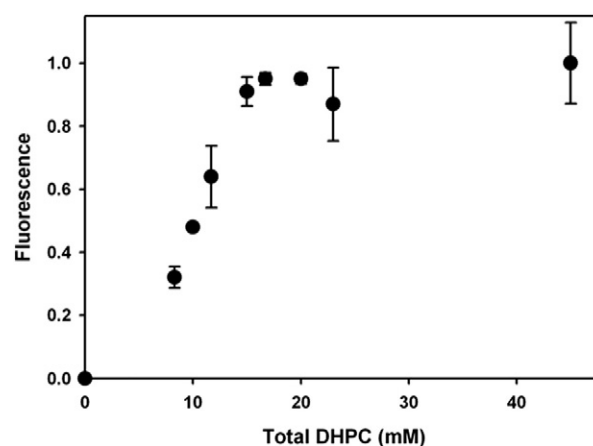


Fig. 2. 1,2-Dihexanoyl-*sn*-glycero-3-phosphocholine (DHPC) concentration effect on the maximum fluorescence after mixing with nanolipoprotein particles (NLPs). NLPs (0.8 μM , containing 2.5 μM 1,2-dimyristoyl-*sn*-glycerol-3-phosphoethanolamine-N-(lissamine rhodamine B sulfonyl) (LR-PE) and 2.6 μM 1,2-di-myristoyl-*sn*-glycerol-3-phosphoethanolamine-N-(7-nitro-2-1,3-benzoxadiazol-4-yl) (NBD)) were reacted in the stopped flow fluorometer with DHPC at the indicated concentration. The final equilibrium value of dequenched NBD fluorescence is shown. Temperature, 23.6 $^{\circ}\text{C}$.



In these equations, L' is an alternative conformation of MSP1E3D1, possibly similar to the “turtle” conformation [8]. Eq. (2) represents a small amount of NLPs slowly dissociating into L' . Eq. (3) shows L' rapidly stripped of lipids by bicelles, B , forming expanded bicelles, B' . Eq. (4) describes the apolipoprotein, L , reacting with NLPs to stimulate the formation of more L' . The rate equation for this scheme has been previously solved [15]. When Eq. (2) is the slowest step, the rate equation predicts a sigmoid time dependence for the formation of B' . Thus, if more apolipoproteins are added to the system, the reaction rate would be expected to increase.

The rate of lipid transfer from NLPs to bicelles is compared to the rate in the presence of a 2.5-fold excess of MSP1E3D1 (Fig. 3). NLPs (2.8 μM) were mixed in the stopped-flow spectrometer with bicelles (15 mM DMPC, approximately 125 μM bicelles) (Fig. 3, lower curve), or with the same concentration of bicelles containing additional 14 μM MSP1E3D1 (Fig. 3, upper curve). The initial velocity increases slightly from 1.2 $\mu\text{M s}^{-1}$ to 1.7 $\mu\text{M s}^{-1}$. According to the autocatalytic model, adding a large amount of apolipoprotein to the reaction should run the reaction in Eq. (4), at least initially, at a high rate, essentially as a first-order reaction. The fitted kinetic constants from the autocatalytic model (Eqs. (2)–(4)) predict that the initial rate should be increased about ten times more than the observed increase. Therefore, the autocatalytic model does not apply to this system.

3.4. Temperature dependence of the NLP–bicelle reaction

DMPC undergoes phase transitions in NLPs and in bicelles, as a function of temperature. In NLPs, DMPC was reported to have a gel-to-liquid crystal phase transition at about 27.5–29 $^{\circ}\text{C}$ [16], above the multilamellar transition temperature of 24 $^{\circ}\text{C}$ [17]. Bicelles display complex phase behavior, but evidence for a bicelle gel-to-liquid crystal transition in the mid-20 $^{\circ}\text{C}$ range has been reported [18]. The relatively slow rates observed for lipid transfer from NLPs to bicelles may reflect the kinetics of the gel phase lipids, but at higher temperature the liquid crystal phase lipids might transfer at a much faster rate. A sharp break would be expected in the Arrhenius plot of a phase transition-dependent kinetic process. Thus, we measured the temperature dependence of the rates of the NLP–bicelle lipid transfer. It should be noted that bicelles having $q \gg 1$ and high total lipid concentrations

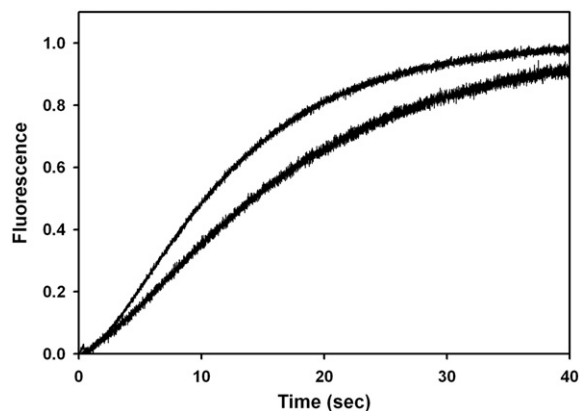


Fig. 3. Effect of added apolipoprotein (MSP1E3D1). Lower curve, 2.8 μM nanolipoprotein particles (5.6 μM MSP1E3D1). Upper curve, additional 14 μM MSP1E3D1 added. Bicelle 1,2-dimyristoyl-*sn*-glycero-3-phosphocholine (DMPC) = 15 mM (about 125 μM bicelles, assuming 120 DMPC/bicelle).

are known to form multi-lamellar phases above 30 $^{\circ}\text{C}$ [2]. In our measurements, the bicelles were in the region of the phase diagram in which no temperature-dependent multi-lamellar phases form [19].

The temperature dependence of the NLP–bicelle reaction is shown in Fig. 4. The traces were fit with Eq. (1). The reaction rate increases substantially at higher temperatures, and at 33 $^{\circ}\text{C}$ the sigmoid shape of the kinetics has changed to exponential. The empirically fitted kinetic constants are shown in Fig. 5 as an Arrhenius plot. The data falls on a single straight line, so there is no evidence for a strong phase transition-dependent break. The slope indicates a strong temperature dependence (activation energy = 28 kcal/mol).

4. Discussion

Our measurements of the rate of lipid transfer from NLPs to bicelles (Fig. 1) show that this reaction is surprisingly slow compared with, for example, detergent transfer between micelles [20]. The rate is in the range of lipid transfer rates between bicelles via through-solution diffusion [21,22]. The diffusional transfer mechanism previously described probably involves micelles, because of the very low water solubility of lipids. However, we found that the transfer of lipids from NLPs to DHPC micelles was faster than we could resolve with our stopped flow kinetics spectrometer. Also, the activation energy for the diffusional mechanism [21–23] is much lower than what we observed for NLP to bicelle lipid transfer (Fig. 5). Thus, it is unlikely that DHPC micelles act as an intermediary in the transfer process (Fig. 2). Near the DMPC

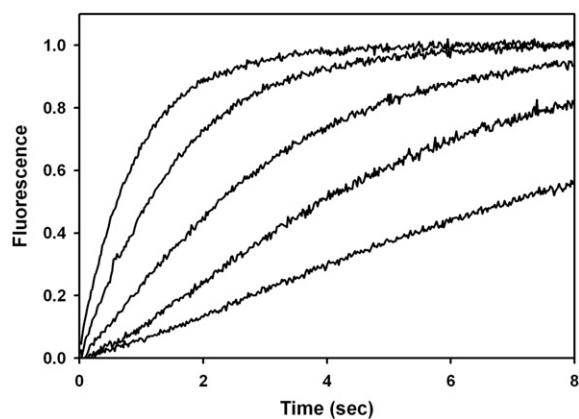


Fig. 4. Effect of temperature on bicelle–nanolipoprotein particle mixing kinetics. Temperatures, from upper to lower curves: 33.2, 30.0, 26.8, 23.6, and 20.5 $^{\circ}\text{C}$. Same concentration conditions as lower curve in Fig. 1.

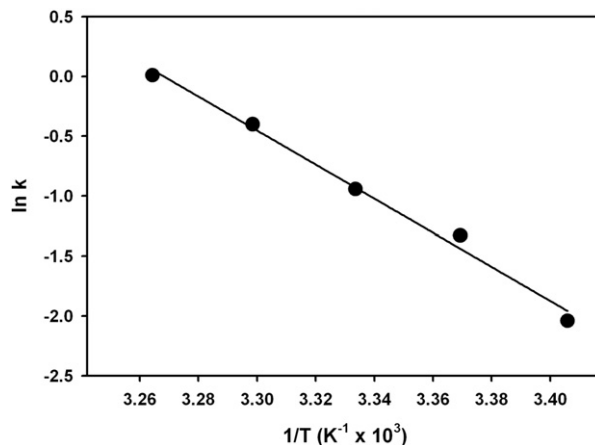


Fig. 5. Arrhenius plot of kinetic constants. Data in Fig. 4 fit with Eq. (1) to obtain pseudo-first-order rate constants.

phase transition temperature, the NLP to bicelle lipid transfer reaction displayed sigmoid kinetics (Fig. 1). This suggests the possibility that the reaction involves autocatalysis, which is known to produce sigmoid reaction rates. Exchangeable apolipoproteins undergo slow conformational changes [24,25], and it is possible to construct an autocatalytic mechanism for lipid transfer involving this (Eqs. (2)–(4)). However, we ruled out the involvement of the NLP apolipoprotein, MSP1E3D1, in autocatalysis of lipid transfer (Fig. 3). From the temperature dependence of the reaction (Fig. 4), we found that there was no sharp change in the rate at the lipid phase transition temperature for DMPC (Fig. 5), which suggests that the lipid gel phase does not cause the slow kinetics or sigmoid shape.

A sigmoid time-dependence of lipid mixing is often observed in membrane fusion via fusion pores. This kinetic feature, called a “lag phase,” has been reported in liposome fusion with virus membranes [26–29], and also in liposome–liposome fusion mediated by peptides [30], phospholipase-generated diacylglycerol [31], clathrin [32], and polyethyleneglycol [33]. A lag phase can occur in a sequential reaction mechanism where the rates of successive steps are similar [34]. The rates of lipid mixing through membrane fusion pores have relatively high activation energies, in the range of 30 kcal/mol [35,36], which is similar to what we observed for the rates of lipid mixing between NLPs and bicelles (Fig. 5). Micelle fusion also was found to have a high activation energy [37], and in some cases lag phase kinetics can occur [34].

The similarity between our observations and the properties of fusion pore lipid mixing kinetics or micelle fusion suggests possible models for the interaction between NLPs and bicelles. In a fusion pore mechanism, the NLP and bicelle discs would interact face-to-face, in a manner similar to the rouleaux often seen in negative stain electron micrographic images of NLPs and high density lipoproteins. DHPC, the short-chain lipid of bicelles, is likely to be present to some extent in the bilayer of the bicelle. The voids created by DHPC could promote the formation of a hemifusion stalk. Subsequently, a fusion pore forms. The pore would rapidly open to form a cylinder: one end edged by the apolipoprotein, and the other end edged by DHPC (see Fig. 6). This structure is similar to that proposed for SNARE-induced pore formation between NLPs and vesicles [38]. The lipids would freely mix in the cylinder. The MSP1E3D1-edged end of the cylinder would be distorted, with a rim of high curvature radius. The DHPC-edged end would have no conformational restrictions, and it could form a straight cylinder. Lipids could quickly exchange at the DHPC end with other bicelles, presumably by collision. Bicelle–bicelle collision was reported to result in fusion into unilamellar vesicles [39], but the bicelles in that study contained high long-chain to short-chain lipid ratios (q) and low total lipid concentration. However, at the lower q levels in the

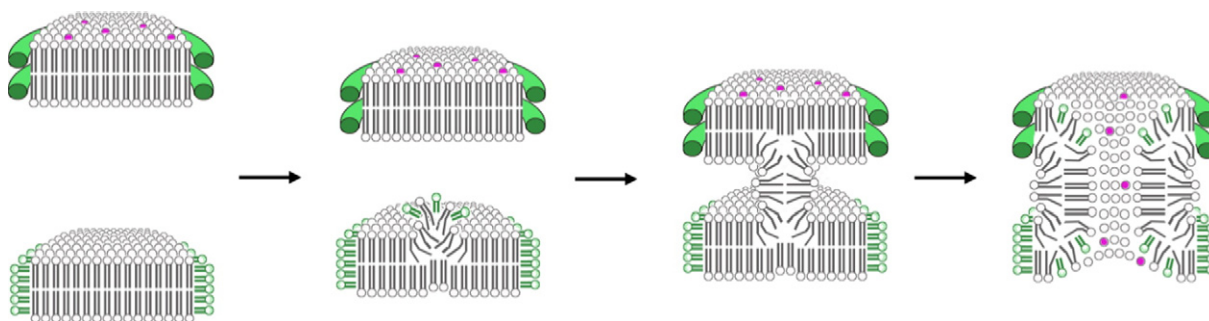


Fig. 6. Fusion pore model for NLP–bicelle lipid mixing. Left: NLP, edged by apolipoprotein MSP1E3D1 (upper disc), containing fluorescent lipids (purple dots), approaches bicelle, edged by (1,2-dihexanoyl-*sn*-glycero-3-phosphocholine) DHPC (lower disc), face-to-face. Middle: DHPC molecules in the bicelle bilayer stimulate the formation of fusion stalk. Right: fusion pore expands to distorted cylinder, and fluorescent lipids diffuse to DHPC edge, from which they can transfer to bicelles by collision.

bicelles used in our experiments, bicelle fusion and fission may be balanced, so the size would remain relatively stable and the only change would be the mixing of the lipids. In an alternative fusion mechanism, a bicelle DHPC edge would transiently fuse with one DMPC bilayer leaflet of an NLP, picking up or leaving long-chain lipids. Then the bicelle and NLP would separate. NLPs are known to display a distribution of different sizes [40,41] presumably reflecting different apolipoprotein conformations [8]. In this model, at the reaction end point the apolipoproteins would still be bound to lipids as NLPs, but they would have smaller diameters, as observed [5], presumably due to the greater stability of bicelles compared with NLPs. These models could be distinguished in future experiments. The addition of fusogenic peptides should increase the rate of the NLP–bicelle lipid mixing via a fusion pore mechanism, but not via the edge-collision mechanism.

The lack of an NLP concentration dependence on the mixing kinetics (Table 1) implies that only a small subset of bicelles are competent to react, so that even at the lowest NLP concentration we tested, all the available bicelle “active sites” were saturated. In the fusion pore mechanism, this might be an indication that a particular statistically rare configuration of DHPC guests within the bicelle’s DMPC bilayer domain is required for hemifusion to occur. Since the bilayer concentration of DHPC is thought to increase in bicelles at higher temperatures [42], a rate dependence on NLP concentration might appear at higher temperatures, where more fusion pore sites would be predicted to form. This predicted temperature effect will be investigated in future experiments.

Acknowledgments

This study is supported in part by the NIH grants R21AI101767 (R.R.) and R25GM096955 (U. Puerto Rico Ponce).

References

- [1] K.J. Glover, J.A. Whiles, G. Wu, N. Yu, R. Deems, J.O. Struppe, R.E. Stark, E.A. Komives, R.R. Vold, Structural evaluation of phospholipid bicelles for solution-state studies of membrane-associated biomolecules, *Biophys. J.* 81 (2001) 2163–2171.
- [2] J. Katsaras, T.A. Harroun, J. Pencir, M.P. Nieh, “Bicellar” lipid mixtures as used in biochemical and biophysical studies, *Naturwiss* 92 (2005) 355–366.
- [3] T.H. Bayburt, S.G. Sligar, Membrane protein assembly into nanodiscs, *FEBS Lett.* 584 (2010) 1721–1727.
- [4] B.A. Chromy, E. Arroyo, C.D. Blanchette, G. Bench, H. Benner, J.A. Cappuccio, M.A. Coleman, P.T. Henderson, A.K. Hinz, E.A. Kuhn, J.B. Pesavento, B.W. Segelke, T.A. Sulchek, T. Tarasow, V.L. Walsworth, P.D. Hoepflich, Different apolipoproteins impact nanolipoprotein particle formation, *J. Am. Chem. Soc.* 129 (2007) 14348–14354.
- [5] G. Lai, R. Renthal, Integral membrane protein fragment recombination after transfer from nanolipoprotein particles to bicelles, *Biochemistry* 52 (2013) 9405–9412.
- [6] F. Katzen, J.E. Fletcher, J.P. Yang, D. Kang, T.C. Peterson, J.A. Cappuccio, C.D. Blanchette, T. Sulchek, B.A. Chromy, P.D. Hoepflich, M.A. Coleman, W. Kudlicki, Insertion of membrane proteins into discoidal membranes using a cell-free protein expression approach, *J. Proteome Res.* 7 (2008) 3535–3542.
- [7] P.A. Luchette, T.N. Vetman, R.S. Prosser, R.E. Hancock, M.P. Nieh, C.J. Glinka, S. Krueger, J. Katsaras, Morphology of fast-tumbling bicelles: a small angle neutron scattering and NMR study, *Biochim. Biophys. Acta* 1513 (2001) 83–94.
- [8] V. Gogonea, G.S. Gerstenecker, Z. Wu, X. Lee, C. Topbas, M.A. Wagner, T.C. Tallant, J.D. Smith, P. Callow, V. Pipich, H. Malet, G. Schoehn, J.A. DiDonato, S.L. Hazen, The low-resolution structure of nHDL reconstituted with DMPC with and without cholesterol reveals a mechanism for particle expansion, *J. Lipid Res.* 54 (2013) 966–983.
- [9] D. Lancet, I. Pecht, Spectroscopic and immunochemical studies with nitrobenzoxadiazolealanine, a fluorescent dinitrophenyl analogue, *Biochemistry* 16 (1977) 5150–5157.
- [10] R. Liu, F.J. Sharom, Proximity of the nucleotide binding domains of the P-glycoprotein multidrug transporter to the membrane surface: a resonance energy transfer study, *Biochemistry* 37 (1998) 6503–6512.
- [11] P.R. Allegrini, H. Sigrist, J. Schaller, P. Zahler, Site-directed fluorogenic modification of bacteriorhodopsin by 7-chloro-4-nitrobenzo-2-oxa-1,3-diazole, *Eur. J. Biochem.* 132 (1983) 603–608.
- [12] A. Andersson, L. Maler, Size and shape of fast-tumbling bicelles as determined by translational diffusion, *Langmuir* 22 (2006) 2447–2449.
- [13] R.A. Alberty, G.G. Hammes, Application of the theory of diffusion-controlled reactions to enzyme kinetics, *J. Phys. Chem.* 62 (1958) 154–159.
- [14] M.P. Nieh, C.J. Glinka, S. Krueger, R.S. Prosser, J. Katsaras, SANS study on the effect of lanthanide ions and charged lipids on the morphology of phospholipid mixtures. Small-angle neutron scattering, *Biophys. J.* 82 (2002) 2487–2498.
- [15] E. Diez-Pena, I. Quijada-Garrido, J.M. Barrales-Rienda, Hydrogen-bonding effects on the dynamic swelling of P(N-iPAAM-co-MAA) copolymers. A case of autocatalytic swelling kinetics, *Macromolecules* 35 (2002) 8882–8888.
- [16] I.G. Denisov, M.A. McLean, A.W. Shaw, Y.V. Grinkova, S.G. Sligar, Thermotropic phase transition in soluble nanoscale lipid bilayers, *J. Phys. Chem. B* 109 (2005) 15580–15588.
- [17] S. Mabrey, J.M. Sturtevant, Investigation of phase transitions of lipids and lipid mixtures by sensitivity differential scanning calorimetry, *Proc. Natl. Acad. Sci. U. S. A.* 73 (1976) 3862–3866.
- [18] E. Stermin, D. Nizza, K. Gawrisch, Temperature dependence of DMPC/DHPC mixing in a bicellar solution and its structural implications, *Langmuir* 17 (2001) 2610–2616.
- [19] L. van Dam, G. Karlsson, K. Edwards, Direct observation and characterization of DMPC/DHPC aggregates under conditions relevant for biological solution NMR, *Biochim. Biophys. Acta* 1664 (2004) 241–256.
- [20] J.D. Bolt, N.J. Turro, Measurement of the rates of detergent exchange between micelles and the aqueous phase using phosphorescent labeled detergents, *J. Phys. Chem.* 85 (1981) 4029–4033.
- [21] J.W. Nichols, Phospholipid transfer between phosphatidylcholine–taurocholate mixed micelles, *Biochemistry* 27 (1988) 3925–3931.
- [22] V.S. Narayanan, J. Storch, Fatty acid transfer in taurodeoxycholate mixed micelles, *Biochemistry* 35 (1996) 7466–7473.
- [23] S.D. Zucker, J. Storch, M.L. Zeidel, J.L. Gollan, Mechanism of the spontaneous transfer of unconjugated bilirubin between small unilamellar phosphatidylcholine vesicles, *Biochemistry* 31 (1992) 3184–3192.
- [24] M. Kono, Y. Okumura, M. Tanaka, D. Nguyen, P. Dhanasekaran, S. Lund-Katz, M.C. Phillips, H. Saito, Conformational flexibility of the N-terminal domain of apolipoprotein A-I bound to spherical lipid particles, *Biochemistry* 47 (2008) 11340–11347.
- [25] C. Mizuguchi, M. Hata, P. Dhanasekaran, M. Nickel, M.C. Phillips, S. Lund-Katz, H. Saito, Fluorescence analysis of the lipid binding-induced conformational change of apolipoprotein E4, *Biochemistry* 51 (2012) 5580–5588.
- [26] T. Stegmann, J.M. White, A. Helenius, Intermediates in influenza induced membrane fusion, *EMBO J.* 9 (1990) 4231–4241.
- [27] T. Shanguan, D. Alford, J. Bentz, Influenza-virus–liposome lipid mixing is leaky and largely insensitive to the material properties of the target membrane, *Biochemistry* 35 (1996) 4956–4965.
- [28] Y. Gaudin, Rabies virus-induced membrane fusion pathway, *J. Cell Biol.* 150 (2000) 601–612.
- [29] F.I. Schmidt, P. Kuhn, T. Robinson, J. Mercer, P.S. Dittrich, Single-virus fusion experiments reveal proton influx into vaccinia virions and hemifusion lag times, *Biophys. J.* 105 (2013) 420–431.

- [30] D. Top, J.A. Read, S.J. Dawe, R.T. Syvitski, R. Duncan, Cell–cell membrane fusion induced by p15 fusion-associated small transmembrane (FAST) protein requires a novel fusion peptide motif containing a myristoylated polyproline type II helix, *J. Biol. Chem.* 287 (2012) 3403–3414.
- [31] M.B. Ruiz-Arguello, G. Basanez, F.M. Goni, A. Alonso, Different effects of enzyme-generated ceramides and diacylglycerols in phospholipid membrane fusion and leakage, *J. Biol. Chem.* 271 (1996) 26616–26621.
- [32] S. Maezawa, T. Yoshimura, Sequence of critical events involved in fusion of phospholipid vesicles induced by clathrin, *Biochim. Biophys. Acta* 1070 (1991) 429–436.
- [33] J. Lee, B.R. Lentz, Evolution of lipidic structures during model membrane fusion and the relation of this process to cell membrane fusion, *Biochemistry* 36 (1997) 6251–6259.
- [34] S. Rasi, F. Mavelli, P.L. Luisi, Cooperative micelle binding and matrix effect in oleate vesicle formation, *J. Phys. Chem. B* 107 (2003) 14068–14076.
- [35] M.J. Clague, C. Schoch, L. Zech, R. Blumenthal, Gating kinetics of pH-activated membrane fusion of vesicular stomatitis virus with cells: stopped-flow measurements by dequenching of octadecylrhodamine fluorescence, *Biochemistry* 29 (1990) 1303–1308.
- [36] J. Lee, B.R. Lentz, Secretory and viral fusion may share mechanistic events with fusion between curved lipid bilayers, *Proc. Natl. Acad. Sci. U. S. A.* 95 (1998) 9274–9279.
- [37] Y. Rharbi, M. Li, M.A. Winnik, K.G. Hahn, Temperature dependence of fusion and fragmentation kinetics of Triton X-100 micelles, *J. Am. Chem. Soc.* 122 (2000) 6242–6251.
- [38] L. Shi, Q.T. Shen, A. Kiel, J. Wang, H.W. Wang, T.J. Melia, J.E. Rothman, F. Pincet, SNARE proteins: one to fuse and three to keep the nascent fusion pore open, *Science* 335 (2012) 1355–1359.
- [39] S. Mahabir, D. Small, M. Li, W. Wan, N. Kucerka, K. Littrell, J. Katsaras, M.P. Nieh, Growth kinetics of lipid-based nanodiscs to unilamellar vesicles—a time-resolved small angle neutron scattering (SANS) study, *Biochim. Biophys. Acta* 1828 (2013) 1025–1035.
- [40] C.D. Blanchette, R. Law, W.H. Benner, J.B. Pesavento, J.A. Cappuccio, V. Walsworth, E.A. Kuhn, M. Corzett, B.A. Chromy, B.W. Segelke, M.A. Coleman, G. Bench, P.D. Hoepflich, T.A. Sulchek, Quantifying size distributions of nanolipoprotein particles with single-particle analysis and molecular dynamic simulations, *J. Lipid Res.* 49 (2008) 1420–1430.
- [41] C.D. Blanchette, J.A. Cappuccio, E.A. Kuhn, B.W. Segelke, W.H. Benner, B.A. Chromy, M.A. Coleman, G. Bench, P.D. Hoepflich, T.A. Sulchek, Atomic force microscopy differentiates discrete size distributions between membrane protein containing and empty nanolipoprotein particles, *Biochim. Biophys. Acta* 1788 (2009) 724–731.
- [42] M.P. Nieh, V.A. Raghunathan, G. Pabst, T. Harroun, K. Nagashima, H. Morales, J. Katsaras, P. Macdonald, Temperature driven annealing of perforations in bicellar model membranes, *Langmuir* 27 (2011) 4838–4847.